



# Studies on the effects of bone marrow stem cells on mitochondrial function and the alleviation of ARDS

Keji Zhang<sup>1</sup> · Yuan Gao<sup>2</sup> · Yuxiao Deng<sup>2</sup> · Xiao Zhou<sup>2</sup> · Changqing Zhu<sup>1</sup> · Zhengyu He<sup>2</sup> · Dan Lv<sup>1</sup>

Received: 22 April 2020 / Accepted: 14 August 2020 / Published online: 26 August 2020  
© Springer Science+Business Media, LLC, part of Springer Nature 2020

## Abstract

Mesenchymal stem cells (MSCs) can alleviate acute respiratory distress syndrome (ARDS), but the mechanisms involved are unclear, especially about their specific effects on cellular mitochondrial respiratory function. Thirty mice were allocated into the Control, LPS, and LPS + Bone marrow mesenchymal stem cell (BMSC) group ( $n = 10/\text{group}$ ). Mouse alveolar epithelial cells (MLE-12) and macrophage cells (RAW264.7) were divided into the same groups. Pathological variation, inflammation-related factors, reactive oxygen species (ROS), ATP levels, and oxygen consumption rate (OCR) were analyzed. Pathologic features of ARDS were observed in the LPS group and were significantly alleviated by BMSCs. The trend in inflammation-related factors among the three groups was the LPS group > LPS + BMSC group > Control group. In the MLE-12 co-culture system, IL-6 was increased in the LPS group but not significantly reduced in the LPS + BMSC group. In the RAW264.7 co-culture system, IL-1 $\beta$ , TNF- $\alpha$ , and IL-10 levels were all increased in the LPS group, IL-1 $\beta$  and TNF- $\alpha$  levels were reduced by BMSCs, while IL-10 level kept increasing. ROS and ATP levels were increased and decreased respectively in both MLE-12 and RAW264.7 cells in the LPS groups but reversed by BMSCs. Basal OCR, ATP-linked OCR, and maximal OCR were lower in the LPS groups. Impaired basal OCR and ATP-linked OCR in MLE-12 cells were partially restored by BMSCs, while impaired basal OCR and maximal OCR in RAW264.7 cells were restored by BMSCs. BMSCs improved the mitochondrial respiration dysfunction of macrophages and alveolar epithelial cells induced by LPS, alleviated lung tissue injury, and inflammatory response in a mouse model of ARDS.

**Keywords** BMSCs · ARDS · Macrophages · Alveolar epithelial cells · Mitochondrial respiratory function · OCR

## Introduction

Acute respiratory distress syndrome (ARDS) is the leading cause of death in ICU patients [1]. ARDS is a severe complication of patients presenting life-threatening organ dysfunction caused by a dysregulated host response to viral (e.g., SARS-CoV-2), bacterial, or fungal infection [2], and about 67% of patients with COVID-19 admitted to the ICU

are diagnosed with ARDS [3]. As a multifactorial syndrome, ARDS involves severe lung injury characterized by hypoxemia, loss of lung compliance, and pulmonary edema [4]. The pathology of ARDS is strongly associated with pulmonary sepsis and can involve a disordered immune response [5]. Neutrophils and macrophages invade the alveolar space and produce high levels of pro-inflammatory cytokines, such as interleukin (IL)-6, IL-1 $\beta$ , IL-8, and tumor necrosis factor-alpha (TNF- $\alpha$ ), resulting in damage to the lung endothelia and epithelia [6]. The production of reactive oxygen species (ROS) resulting from the increased inflammation impairs lung barrier function and increases vascular permeability [7].

As there are no direct therapies for ARDS, treatment relies on management strategies such as protective mechanical ventilation and fluid-restriction [8]. This, however, can increase the inflammatory response and cause ventilator-induced lung injury [9]. Even antibiotic treatment cannot often reduce the inflammatory response despite the removal

✉ Yuan Gao  
shsmubs@163.com

✉ Yuxiao Deng  
dengyuxiao@renji.com

<sup>1</sup> Department of Emergency, Ren Ji Hospital, School of Medicine, Shanghai Jiao Tong University, Shanghai 200127, China

<sup>2</sup> Department of Critical Care Medicine, Ren Ji Hospital, School of Medicine, Shanghai Jiao Tong University, Shanghai 200127, China

of the causative pathogen [4]. Other pharmacologic treatments, including glucocorticoids, surfactants, inhaled nitric oxide, antioxidants, and protease inhibitors, have been ineffective so far [10].

Mesenchymal stem cells (MSCs) are an emerging treatment method [11–13]. MSCs have a protective effect on sepsis-induced ARDS. Previous studies showed that MSCs could improve oxygenation and reduce the histological changes of lung injury in the treatment of sepsis-induced ARDS [14, 15], but the specific mechanism of action is not very clear. MSCs play a role in the immune modulation of immune cells, including alveolar macrophages, through paracrine action and cell contact [16, 17]. Alveolar macrophages and alveolar epithelial cells are important cells found in the lung and play roles in the immunity of this organ [18]. Apoptosis caused by the excessive activation of alveolar macrophages is an important pathogenesis mechanism of ARDS [19]. Cell apoptosis can be caused by a mitochondrion-dependent pathway [20, 21]. The functional status of alveolar macrophage mitochondria is an important factor affecting the release of interferon (IFN)- $\gamma$ , TNF- $\alpha$ , IL-1 $\beta$ , and IL-6 by alveolar macrophages [22]. LPS stimulation can cause the abnormal mitochondrial function of alveolar macrophages and increased intracellular ROS content [23]. MSCs can prolong the survival time of cells under ischemia and hypoxia [24]. MSCs can reduce reactive oxygen species (ROS) production by alveolar macrophages [20, 21]. MSCs might improve mitochondrial dysfunction of alveolar macrophages induced by lipopolysaccharide (LPS).

These studies indirectly suggest that mesenchymal stem cells may improve the mitochondrial dysfunction of alveolar macrophages caused by LPS stimulation. Nevertheless, how MSCs affect the specific changes in the mitochondrial respiratory function of alveolar macrophages induced by LPS is not well understood. In addition, it is not clear how MSCs affect the specific changes in the mitochondrial respiratory function of the alveolar epithelial cells injured by LPS. We hypothesized that MSCs improve the mitochondrial respiratory function of alveolar macrophages and alveolar epithelial cells, increase the ATP levels in alveolar macrophages, and decrease ROS levels in alveolar macrophages, thereby improving cell dysfunction and ultimately alleviating sepsis-induced ARDS. Therefore, in this study, we performed cell experiments to evaluate cell metabolism, cell respiration, mitochondrial function, and changes in ROS levels. Furthermore, we established a mouse model of LPS-induced ARDS to observe the pathological changes in lung tissues and in the concentrations of inflammatory factors in lung tissue and alveolar lavage fluid. The results of this study should provide a solid theoretical basis for the clinical application of MSCs in the treatment of sepsis-induced acute lung injury. Mouse models have been used extensively in the study of ARDS [25]. These have provided some insight into the mechanisms

involved. A common method is the use of LPS to model sepsis-induced ARDS. This model causes lung injury within hours of LPS challenge, peaking within 24–36 h and followed by a rapid recovery phase over the next 2–3 days [26, 27].

## Materials and methods

### Animals

C57bl/6j wild-type male mice were purchased from Shanghai Sippr-bk Laboratory Animal Ltd. The mice used for isolating the BMSCs were 2–3 weeks old (12–14 g). The mice used for ARDS modeling were 8–10 weeks old (25–28 g). The animals were kept in a specific pathogenic-free and laminar flow laboratory cage with controlled temperature and humidity and a 12-h light/dark cycle. All animal protocols were approved by the Institutional Animal Care and Use Committee of Ren Ji Hospital (IACUC Approval Number RJ2019-0210). All experiments were in accordance with the National Institutes of Health Guidelines for the Care and Use of Laboratory Animals.

### Isolation of BMSC cells

BMSCs were isolated and passaged for in vivo or in vitro experiments. The BMSCs were isolated from five C57bl/6j male mice aged 2–3 weeks (Shanghai Sippr-bk Laboratory Animal Ltd.) according to previously developed procedures [28]. The mice were anesthetized with 5% chloral hydrate (0.1 ml/10 g) before sacrifice by cervical dislocation and washed in a wide-mouth cup containing 100 ml 70% alcohol for 3 min. Then the mice were placed in a 100-mm sterile glass dish, the inguinal skin was cut, the muscles were dissected, and the femurs under the femoral head were cut to separate the lower limbs from the trunk. Subsequently, the forelimbs at the armpits were cut, and the humeri were separated. The skin was peeled off, and micro-dissecting scissors were used to remove the muscles and tendons from the humeri, tibiae, and femurs. The bones were placed on sterile gauze and rubbed carefully to remove the attached soft tissues. Prior to treatment, the bones were immersed in a 35-mm sterile glass dish in 5 ml of  $\alpha$ -minimal essential media (MEM, Gibco, USA) containing 0.1% penicillin/streptomycin and 2% FBS (Hyclone, USA). The bones were not stored for more than 2 h. Hematopoietic cells were isolated from the tibiae and femurs after the callus at the ends of the bone marrow cavity was removed using sterile scissors. Then a 0.45-mm syringe needle was inserted into the bone marrow cavity, through which 3 ml of  $\alpha$ -MEM was injected to flush out the bone marrow. The bone marrow cavity was

thoroughly rinsed with a syringe at least three times until the bones turned white.

The humeri, femurs, and tibiae were held with forceps, and the dense bones were cut into 1–3-mm<sup>3</sup> fragments with scissors, placed into a 25-cm<sup>2</sup> plastic culture bottle, and suspended in 3 ml of  $\alpha$ -MEM (containing 10% FBS and 1 mg/ml collagenase II), followed by digestion for 1–2 h in a shaking incubator at 37 °C at a speed of 200 rpm. The digestion was stopped when the small bone fragments were loosely connected to each other. The digestion medium and released cells were aspirated and discarded. The bone pieces were washed three times with 6 ml of  $\alpha$ -MEM containing 10% FBS (Hyclone, USA), followed by incubation and inoculation for 3 days in a 5% CO<sub>2</sub>, 37 °C incubator (Forma Scientific, USA). On the third day after inoculation, the medium was replaced to remove non-adherent cells and tissue debris, using 6 ml of  $\alpha$ -MEM containing 10% FBS over 5 min. During the first three days of inoculation, frequent and unnecessary movements of the bottle were avoided to reduce damage to the sprouting MSCs in the bone fragments. After 5 days, the medium was removed, and 3 ml of a 0.25% trypsin/0.02% EDTA (Gibco, USA) solution was added. The cells were digested for 3 min at room temperature (18–25 °C) and passaged at a ratio of 1:3. The cells and bone fragments were re-inoculated in the same bottle to allow BMSCs to continue to migrate from the bone fragments to the bottle for at least 3 days. The medium was changed every 48 h, and the cells were passaged twice a week, at a ratio of 1:4 or 1:3 until the tenth passage. Cells at the 3–8th passage were used for the *in vivo* and *in vitro* experiments.

The 3rd to 5th generations of BMSCs were rinsed with PBS (Gibco, USA) and removed by 0.25% trypsin digestion. The digestion was observed under a microscope and was stopped by Dulbecco's modified Eagle media (DMEM) containing 10% FBS when the cells were detached, followed by the collection of the cell suspension. The suspension was centrifuged at 1000×*g* for 5 min, the supernatant was discarded, and the cell pellets were resuspended with 1% BSA and transferred to centrifuge tubes, with 10<sup>6</sup> cells in each tube.

### Mouse models of ARDS

The C57BL/6J male mice were kept for 1 week before the experiments. LPS dose testing was also performed in mice by allocating animals to three groups: one mouse was assigned to the PBS control group, three mice were assigned to the 10-mg/kg LPS treatment group, three mice were assigned to the 15-mg/kg LPS treatment group, and three mice were assigned to the 20-mg/kg LPS treatment group. After treatment, the animals were placed in different cages

and were housed and fed normally. Testing was performed 48 h later.

For ARDS modeling, the animals were numbered and randomly grouped into the Control, LPS, and LPS + BMSC groups. There were 10 animals in each group. The control group received an intraperitoneal injection of PBS. The LPS group received an intraperitoneal injection of LPS for 30 min, and each animal was injected with PBS (100  $\mu$ l) via the tail vein. The LPS + BMSC group received an intraperitoneal injection of LPS for 30 min and was injected with 100  $\mu$ l of 5 × 10<sup>5</sup> BMSC cells via the tail vein. LPS (Sigma, USA) was dissolved in normal saline to 0.5 mg/ml before use, and the mice in the ARDS groups received 15 mg/kg.

### Analysis of alveolar lavage and lung tissues of mice in the ARDS model

In each group, five mice were selected for bronchoalveolar lavage. The mice that survived 48 h were sacrificed by spinal dislocation, and the trachea was exposed. The chest was opened, the left bronchus was ligated, and then the chest was simply sutured. A small opening was made on the trachea, through which a retention needle was inserted until half of the length, and the needle was fixed with ligature thread. Normal saline (0.5 ml) was drawn into a syringe, which was connected to the retention needle to inject the normal saline into the lung until the entire lung was filled with fluid. The chest was gently massaged for 20 s, retained for 1 min, and then the normal saline was aspirated. The retrieved fluid (about 400  $\mu$ l) was placed in centrifuge tubes on ice. The collected bronchoalveolar lavage fluid (BALF) was centrifuged at 1000 rpm, the precipitate was removed, and the supernatant was collected for ELISA. The right lung tissues were ground and centrifuged; the supernatant was collected, followed by BCA quantification, and ELISA. The left lung tissues were fixed with formalin for histochemistry. For the remaining five mice in each group, the entire lungs were harvested, weighed, and dried overnight in a drying oven (GZX-9023MBE, Shanghai Boxun Industrial Co., Ltd. Medical Equipment Factory, China) and their dry weight was measured the next day.

The levels of IL-1 $\beta$ , TNF- $\alpha$ , and IL-10 in the BALF and lung tissue (right lung) were measured by ELISA assays (Shanghai Enzyme-Linked Biotechnology Co., Ltd., China). In addition, left lung sections were prepared for hematoxylin and eosin (HE) staining with an HE Kit (Thermo, USA). The lung sections were examined to score lung injury using a light microscope (DM750, Leica, Germany). The pathological sections were observed by independent pathologists who were unaware of grouping. Ten high-power fields were selected for each mouse, in which the percentages of the lesion area was evaluated according to the criteria of lung injury score. Then, the mean value of the 10 fields was

calculated according to the area standard of lung injury score, and scores of various criteria were summed up to obtain the lung injury score. The scoring indicators (referring to Smith scoring) were as follows: pulmonary edema, alveolar and mesenchymal congestion, alveolar and mesenchymal inflammation, atelectasis, and formation of the transparent membrane were graded as 0 = no injury; 1 = mild injury (25%); 2 = moderate injury (25–50%); 3 = severe injury (50–75%); 4 = extremely severe injury (75% or more).

### Alveolar epithelial cell or macrophage cell co-culture with BMSCs

The mouse alveolar epithelial cells (MLE-12 cell line, FH1103, FuHeng Cell Center, Shanghai, China) and mouse macrophage cells (RAW264.7 cell line, SCSP-5036, Chinese Academy of Sciences Cell Bank, Shanghai, China) were randomly divided into three groups: the Control group, LPS group, and LPS + BMSC group, with three samples in each group. Then,  $6 \times 10^5$  of MLE-12 cells or RAW264.7 cells were seeded overnight in each well, and  $1 \times 10^5$  of BMSCs were seeded on the upper chamber of 24-well culture plates with Transwell inserts (Corning, USA). PBS was used in the control group, and an indirect co-culture model was adopted. The lower chamber contained 2 ml of serum-free medium. The upper chamber contained 1 ml of serum-free medium or 3 ml for the Control and LPS groups. The measurements were taken after 24 h of stimulation with 0.5  $\mu\text{g}/\text{ml}$  LPS (Sigma, USA).

### Analysis of inflammation

For the analysis of the inflammatory factors, 1 ml of supernatant was collected from each sample and centrifuged. The supernatant was collected for ELISA using kits for IL-6, IL-1 $\beta$ , IL-10, and TNF- $\alpha$  (Shanghai Enzyme-linked Biotechnology Co., Ltd., China). The plates were read on a microplate reader (MuLTiSKAN MK318, Thermo, USA).

Currently, it is believed that alveolar epithelial cells are not a source of IL-1 $\beta$ , IL-10, or TNF- $\alpha$ , but can be a source of IL-6. Therefore, only IL-6 was detected in alveolar epithelial cells to represent the changes in inflammation. Since macrophages are a source of IL-1 $\beta$ , IL-10, and TNF- $\alpha$ , those cytokines were tested in the macrophage co-culture system.

### Analysis of mitochondrial respiratory function

The changes in the mitochondrial respiratory function of the mouse alveolar epithelial cells (MLE-12 cell line) and mouse macrophage cells (RAW264.7 cell line) in each group were tested using the Seahorse detection system (Seahorse XF96 bioenergy analyzer, Agilent, USA). After mounting, the following interventions were, respectively, applied to the

three groups. The extracellular fluid of the corresponding culture system was added before detection according to different intervention conditions. The detection solution was injected three times, including 1  $\mu\text{mol}/\text{l}$  oligomycin, 1  $\mu\text{mol}/\text{l}$  carbonyl cyanide phospho-(p)-trifluoromethoxy phenylhydrazide (FCCP, a proton gradient uncoupler), and 0.5  $\mu\text{mol}/\text{l}$  rotenone/antimycin. The oxygen consumption rate (OCR) value tested before starting the injection of oligomycin was considered as the basal oxygen consumption. The OCR was tested at three time points between each injection point and the next injection point, and the mean value was considered as the OCR at the corresponding period. BCA was used to determine the protein concentration, and the OCR value was corrected by the cell protein concentration.

### ATP measurement

ATP was detected in the alveolar cells by catalyzing luciferin to produce fluorescence with the enhanced ATP test kit (S0027) (Beyotime Biotechnology Co., Ltd., China). The protein concentration was determined by a BCA protein assay kit (Beyotime Biotechnology Co., Ltd., China). The intracellular ATP was isolated as follows: the culture medium was aspirated, and the cells were rinsed twice with pre-cooled PBS and lysed by adding 200  $\mu\text{l}$  of the lysate (equivalent to 1/10 of 2 ml cell culture medium) to each well of the 6-well plate. In order to ensure sufficient pyrolysis, a pipette was used to repeatedly blow or shake the culture plate to ensure complete contact between lysate and cells. The pyrolysis was performed on ice. After that, the cells were centrifuged at 4  $^{\circ}\text{C}$  12,000  $\times g$  for 5 min, and the supernatant was collected for subsequent determination by comparison with an ATP standard curve. Appropriate amounts of ATP working fluid was prepared by applying 100  $\mu\text{l}$  of ATP working fluid to each sample or standard. The reagents were melted in an ice bath. An appropriate amount of ATP reagent was diluted using the ATP reagent dilution solution at a ratio of 1:4. The diluted ATP reagent was the working fluid for subsequent experiments. The ATP working fluid was temporarily stored in an ice bath. ATP concentration was determined by 100  $\mu\text{l}$  of ATP working solution being added to the test well or test tube, which was placed still for 3–5 min at room temperature to remove background ATP. Then, 20  $\mu\text{l}$  of sample or standard was added to the test well or test tube and mixed quickly. A microplate reader was used to test the RLU or CPM after at least 2 s.

### Analysis of ROS

ROS were detected in alveolar epithelial cells using an enhanced ROS test kit (S0033) (Beyotime Biotechnology Co., Ltd.), which uses a fluorescent probe

dichloro-dihydro-fluorescein diacetate (DCFH-DA) to monitor the changes in ROS.

## Flow cytometry

Flow cytometry was used to determine the characteristics of the isolated and passaged BMSCs. A BD-C6 flow cytometer was used. The cells were probed before analysis with CD29-APC, CD90-PE, and CD45-FITC antibodies (Biolegend, USA). In brief, a cell suspension was collected, centrifuged at 1000 rpm for 5 min, the supernatant was discarded, and the cells were resuspended with PBS and adjusted to a concentration of  $5 \times 10^5$ /ml. Each sample was resuspended in 300  $\mu$ l of PBS, and 3  $\mu$ l of antibody was added and mixed gently. The cells were incubated for 20 min at room temperature in the dark, rinsed three times with PBS, and resuspended with 500  $\mu$ l of PBS.

## Statistical analysis

The results were analyzed using SPSS 19.0 (IBM Corp., USA) and analysis of variance (ANOVA) and expressed as mean  $\pm$  standard deviation (SD). A *P*-value  $< 0.05$  was considered significant. Bar charts and line charts were drawn using GraphPad Prism (GraphPad Software, LLC, USA).

## Results

### Flow cytometry and morphological features of the isolated BMSCs

The results of the flow cytometry analysis showed that the isolated BMSCs were CD45<sup>−</sup>CD29<sup>+</sup>CD90<sup>+</sup>. Microscopy showed that the spindle-shaped, triangular, and polygonal cells BMSCs possessed morphologically homogenous fibroblast-like features (Fig. 1).

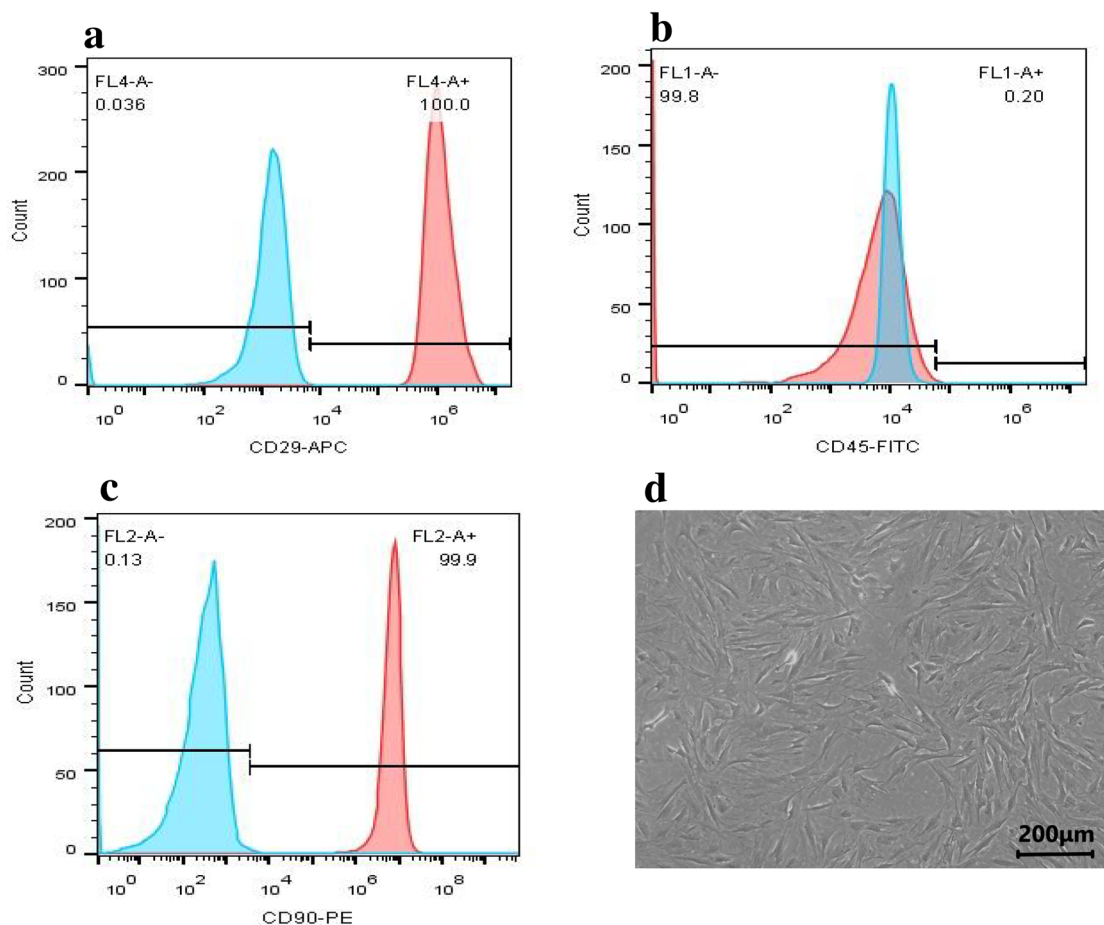


**Fig. 1** Flow cytometry analysis and morphological characteristics of the isolated bone marrow stem cells (BMSCs). **a** Detection of CD29. **b** Detection of CD45. **c** Detection of CD90. Blue refers to the negative control group, and red refers to the sample group. Therefore,

the isolated BMSCs were characterized as CD45<sup>−</sup>CD29<sup>+</sup>CD90<sup>+</sup>. **d** Morphological features of the fourth-generation BMSCs. (Color figure online)

## Histopathology of the mouse ARDS model

The mouse ARDS model was established after intraperitoneal injection of LPS, leading to significant edema and infiltration of inflammatory cells in the lungs. The dosing test showed that pulmonary edema and infiltration of inflammatory cells in the 15 mg/kg LPS dose group were more significant than those in the 10 mg/kg LPS dose group, while all the mice in the 20 mg/kg LPS treatment died within 48 h. So, 15 mg/kg was used as the dose of LPS for the mouse ARDS modeling in this study.

As shown in Fig. 2, the lung sections from the LPS group showed obvious pulmonary edema, thickening, congestion, inflammatory cell infiltration of the alveolar and mesenchyme, local atelectasis, and formation of a membrane. The LPS + BMSC group also showed pulmonary edema, thickening, and inflammatory cell infiltration of the alveolar and mesenchyme, but the severity of lung injury was significantly alleviated compared with the LPS group. The lung injury scores in the Control, LPS, and LPS + BMSC groups were  $0.6 \pm 0.6$ ,  $6.2 \pm 1.9$ , and  $4.4 \pm 0.9$ , respectively ( $P < 0.001$ ). The lung injury score was the highest in the

LPS group, followed by the LPS + BMSC and Control groups ( $P < 0.05$ ). The lung wet-dry weight ratios in the Control, LPS, and LPS + BMSC groups were  $1.97 \pm 0.15$ ,  $12.89 \pm 6.83$ , and  $3.04 \pm 0.85$ , respectively ( $P = 0.002$ ). The Control and LPS + BMSC groups had lower lung wet-dry weight ratios than the LPS group ( $P < 0.05$ ), but without difference between the Control and LPS + BMSC groups ( $P = 0.679$ ).

## Expression of inflammatory factors in lung tissue and BALF samples

Figure 3 shows the expression of inflammatory factors in mouse lung tissue and BALF samples. The IL-1 $\beta$  levels in lung tissues in the Control, LPS, and LPS + BMSC groups were  $52.34 \pm 6.20$ ,  $202.94 \pm 22.66$ , and  $783.94 \pm 15.98$ , respectively ( $P < 0.001$ ). The IL-1 $\beta$  level in the LPS group was higher than that in the LPS + BMSC group, which was higher than in the Control group (all  $P < 0.05$ ).

The TNF- $\alpha$  levels in the lung tissue in the Control, LPS, and LPS + BMSC groups were  $384.18 \pm 145.47$ ,  $645.08 \pm 55.39$ , and  $453.24 \pm 58.90$ , respectively ( $P = 0.003$ ).

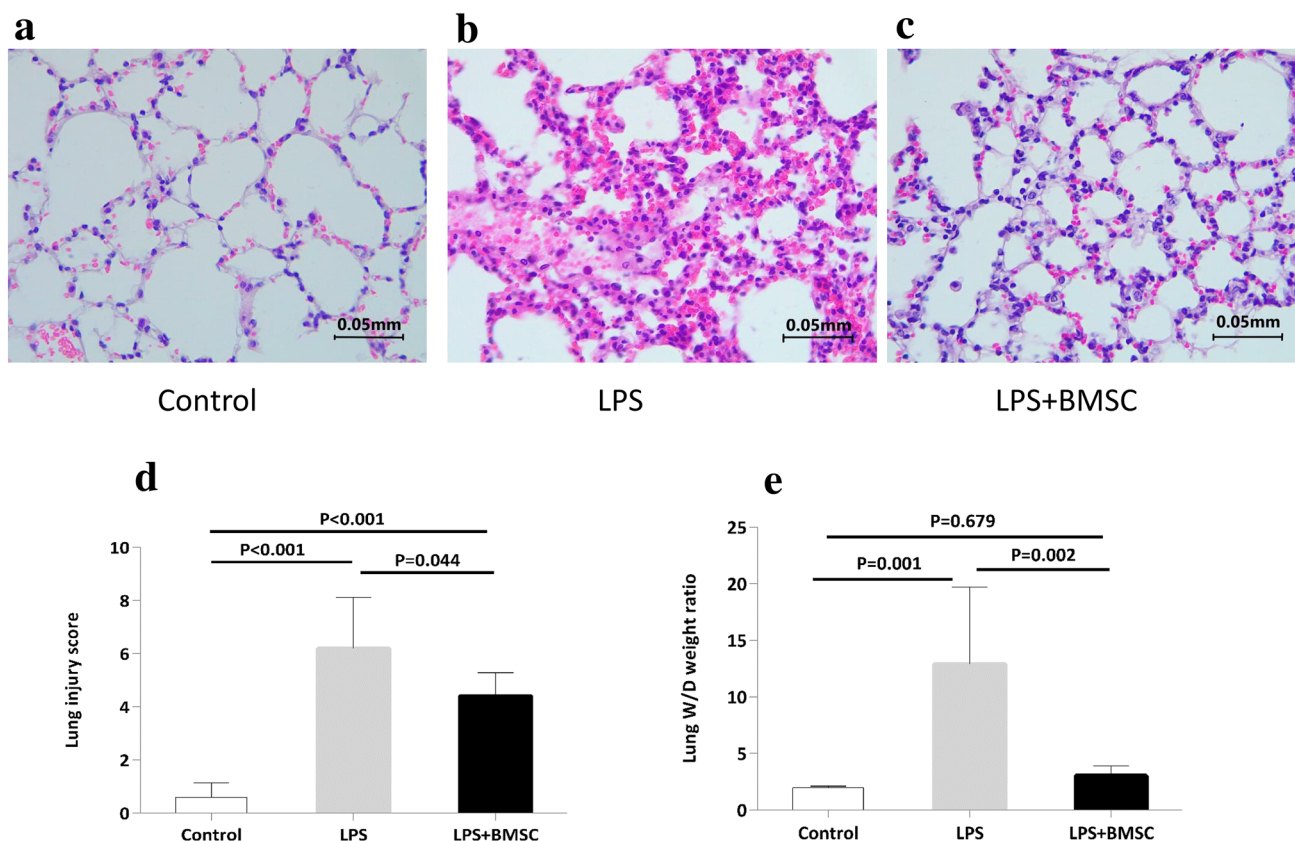


**Fig. 2** Histopathology of LPS-induced lung injury in mice in high-power fields ( $\times 400$ ). **a** Representative lung section from the Control group. **b** Representative lung section from the LPS group. **c** Repre-

sentative lung section from the LPS + BMSC group. **d** Assessment of the lung injury score. **e** The lung wet-dry weight ratio in the Control, LPS, and LPS + BMSC groups

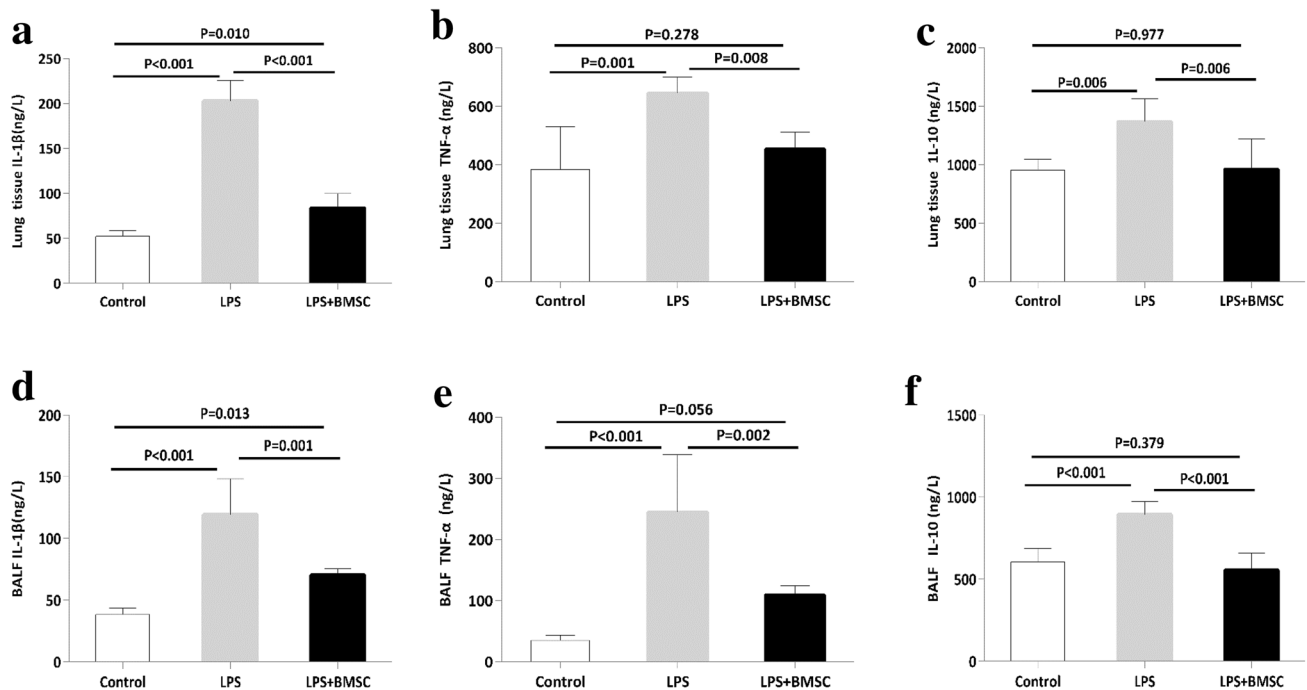


**Fig. 3** Expression of inflammatory factors in mouse lung tissue and bronchoalveolar lavage fluid (BALF) samples. **a** The IL-1 $\beta$  levels in lung tissues in the Control, LPS, and LPS+BMSC groups. **b** The TNF- $\alpha$  levels in lung tissue in the Control, LPS, and LPS+BMSC. **c** The IL-10 levels in lung tissue in the Control, LPS, and LPS+BMSC

groups. **d** The BALF IL-1 $\beta$  in the Control, LPS, and LPS+BMSC groups. **e** The BALF TNF- $\alpha$  in Control, LPS, and LPS+BMSC groups. **f** The BALF IL-10 in the Control, LPS, and LPS+BMSC groups

The Control and LPS+BMSC groups had lower TNF- $\alpha$  than the LPS group ( $P < 0.05$ ), but there was no significant difference between the Control and LPS+BMSC groups ( $P = 0.278$ ).

The IL-10 levels in lung tissue in the Control, LPS, and LPS+BMSC groups were  $956.58 \pm 89.31$ ,  $1367.25 \pm 199.14$ , and  $960.20 \pm 258.32$ , respectively ( $P = 0.008$ ). The Control and LPS+BMSC groups had lower IL-10 than the LPS group ( $P < 0.05$ ), but there was no significant difference in IL-10 in the lung tissue between the Control and LPS+BMSC groups ( $P = 0.977$ ).

The BALF IL-1 $\beta$  levels in the Control, LPS, and LPS+BMSC groups were  $38.46 \pm 5.05$ ,  $119.26 \pm 29.16$ , and  $70.26 \pm 5.37$ , respectively ( $P < 0.001$ ). The LPS group had higher levels of IL-1 $\beta$  in BALF than the LPS+BMSC group, which had higher levels than the Control group ( $P < 0.005$ ).

The lung BALF TNF- $\alpha$  in the Control, LPS, and LPS+BMSC groups were  $35.15 \pm 8.66$ ,  $244.49 \pm 93.89$ , and  $109.12 \pm 15.59$ , respectively ( $P < 0.001$ ). The Control and LPS+BMSC groups had lower lung BALF TNF- $\alpha$  than the LPS group ( $P < 0.05$ ), but there was not a significant difference in lung BALF TNF- $\alpha$  between the Control and LPS+BMSC groups ( $P = 0.056$ ).

The BALF IL-10 in the Control, LPS, and LPS+BMSC groups were  $605.57 \pm 81.18$ ,  $893.65 \pm 80.54$ , and

$554.11 \pm 103.43$ , respectively ( $P \leq 0.001$ ). The Control and LPS+BMSC groups had lower levels than the LPS group ( $P < 0.05$ ), but there was no significant difference between the Control and LPS+BMSC groups ( $P = 0.379$ ).

### Expression of LPS-induced inflammatory factors in extracellular fluid from macrophages and alveolar epithelial cell lines co-cultured with BMSCs

The results of the ELISA analysis for the levels of inflammatory factors in the extracellular fluid produced by alveolar epithelial cells and macrophages are shown in Fig. 4. The IL-6 levels in the MLE-12 cell supernatants in the Control, LPS, and LPS+BMSC groups were  $75.61 \pm 51.63$ ,  $218.09 \pm 43.40$ , and  $173.36 \pm 45.99$ , respectively ( $P = 0.026$ ). The LPS and LPS+BMSC groups had higher IL-6 concentrations than the Control group ( $P < 0.05$ ), but there was no significant difference between the LPS and LPS+BMSC groups ( $P = 0.289$ ). This result suggests that co-culture with BMSC does not directly affect the levels of inflammatory factors secreted by LPS-induced alveolar epithelial cells.

The levels of IL-1 $\beta$  in macrophage supernatants in the Control, LPS, and LPS+BMSC groups were  $11.34 \pm 1.33$ ,  $41.63 \pm 2.39$ , and  $27.92 \pm 0.38$ , respectively ( $P < 0.001$ ). The IL-1 $\beta$  concentration was the highest in the LPS

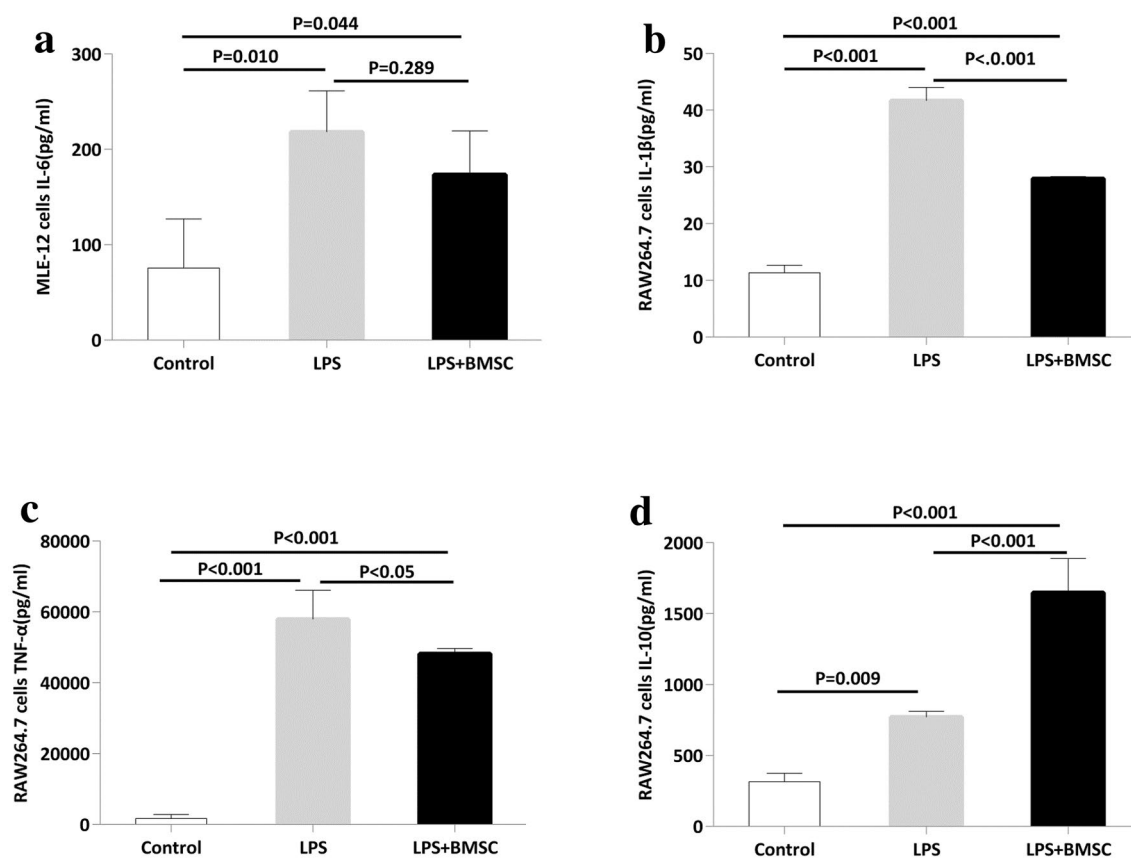


**Fig. 4** Effects of bone marrow stem cells (BMSCs) on lipopolysaccharide (LPS) induced inflammatory factors in macrophage and alveolar epithelial extracellular fluid. **a** IL-6 levels in alveolar epithelial cell (MLE-12) supernatants in the Control, LPS, and LPS+BMSC groups. **b** IL-1 $\beta$  in macrophage (RAW264.7) supernatants in the Control, LPS, and LPS+BMSC groups. **c** TNF- $\alpha$  levels in the RAW264.7 supernatants in the Control, LPS, and LPS+BMSC groups. **d** IL-10 concentration in supernatants from RAW264.7 cells in the Control, LPS, and LPS+BMSC groups

group, followed by the LPS + BMSC and Control groups ( $P < 0.001$ ). The TNF- $\alpha$  levels in the macrophage supernatants in the Control, LPS, and LPS + BMSC groups were  $1713.12 \pm 1134.47$ ,  $57,928.62 \pm 8202.23$ , and  $48,193.64 \pm 1484.96$ , respectively ( $P < 0.001$ ). The LPS group had a higher concentration than the LPS + BMSC group, which had a higher concentration than the Control group ( $P < 0.05$ ). These results suggest that co-culturing macrophages with BMSCs can significantly decrease the concentration of LPS-induced pro-inflammatory factors in the extracellular fluid.

The IL-10 levels in supernatants from RAW264.7 cells in the Control, LPS, and LPS + BMSC groups were  $315.62 \pm 59.56$ ,  $770.52 \pm 41.78$ , and  $1646.88 \pm 241.70$ , respectively ( $P < 0.001$ ). The LPS + BMSC group had a higher concentration than the LPS group, which had a higher concentration than the Control group ( $P < 0.05$ ). This result suggests that the anti-inflammatory IL-10 increases with LPS induction, possibly in response to the

increased inflammation, and increases even further when the macrophages are co-cultured with BMSCs.

### ROS and mitochondrial function in macrophages co-cultures with BMSCs

The analysis of ROS is shown in Fig. 5. The DCFH-DA fluorescence suggested that ROS may be involved in LPS-induced stress in macrophages. The fluorescence signal was higher in the LPS group than in the control and LPS + BMSC groups. The fluorescence signal was also higher in the LPS + BMSC group had more green fluorescence than in the Control group. This demonstrated that LPS caused an elevation of ROS levels in macrophages and that BMSCs reduced LPS-induced ROS generation.

The ATP concentrations in the Control, LPS, and LPS + BMSC groups were  $11.79 \pm 0.84$ ,  $5.52 \pm 0.77$ , and  $8.74 \pm 0.66$ , respectively. The relative ATP levels in the Control, LPS, and LPS + BMSC groups were  $6.25 \pm 0.73$ ,



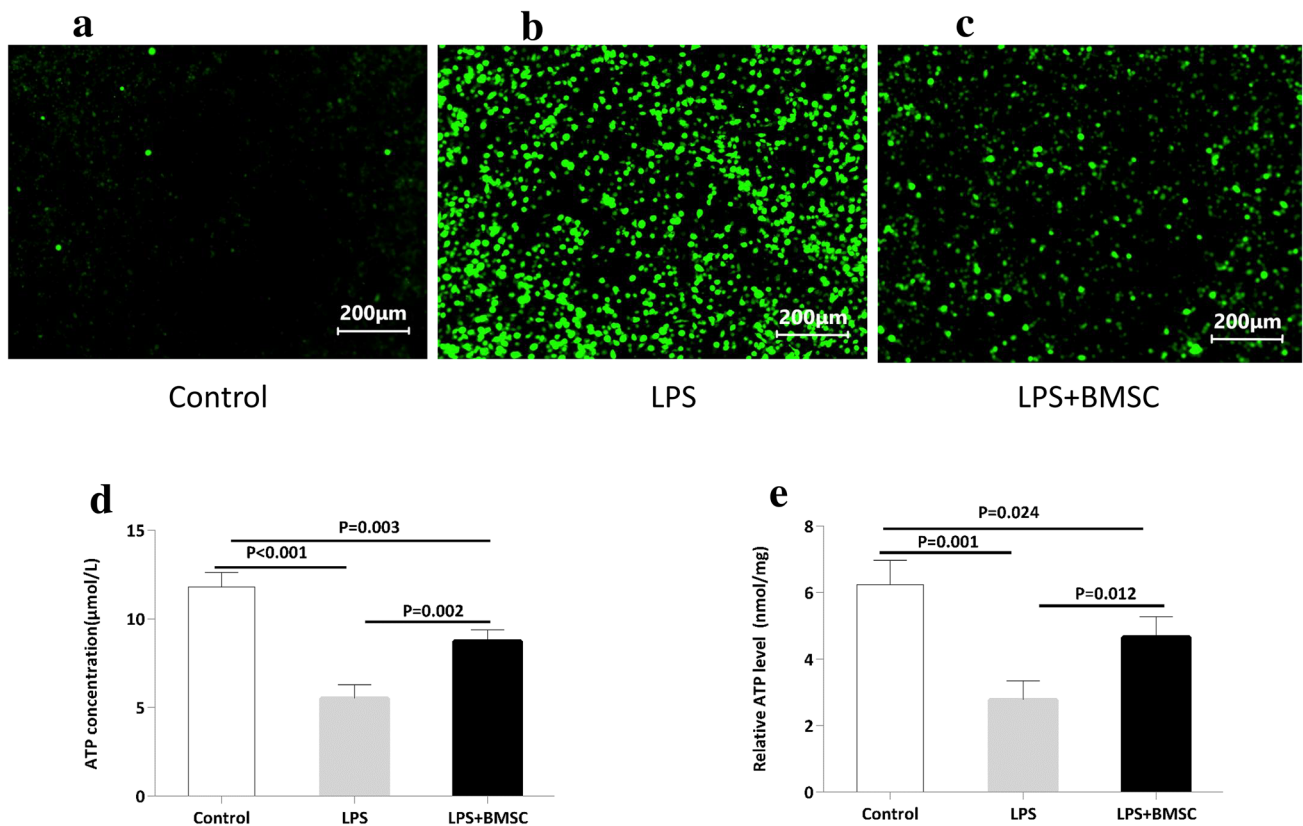


**Fig. 5** Effects of bone marrow stem cells (BMSCs) on changes in lipopolysaccharide (LPS) induced reactive oxygen species (ROS) and mitochondrial function in alveolar macrophages. **a–c** ROS level shown as green fluorescence in macrophages in the Control, LPS,

and LPS + BMSC groups. **d** and **e** Mitochondrial function in the macrophages in the Control, LPS, and LPS + BMSC groups from ATP analysis. (Color figure online)

$2.78 \pm 0.57$ , and  $4.65 \pm 0.63$ , respectively ( $P = 0.002$ ). The relative ATP levels were the highest in the Control group, followed by the LPS + BMSC and the LPS groups ( $P < 0.05$ ).

### Changes in mitochondrial respiratory function induced by LPS in macrophages co-cultured with BMSCs

The analysis of the mitochondrial respiratory function in macrophages is shown in Fig. 6. The three groups showed changes in OCR over time. The mitochondrial basal OCRs in the Control, LPS, and LPS + BMSC groups were  $656.89 \pm 78.76$  pmol/min/10,000 cells,  $452.44 \pm 57.75$  pmol/min/10,000 cells, and  $702.33 \pm 8.67$  pmol/min/10,000 cells, respectively ( $P = 0.004$ ). The Control and LPS + BMSC groups had higher basal OCR than the LPS group ( $P < 0.05$ ), but there was no significant difference between the Control and LPS + BMSC groups ( $P = 0.363$ ).

The ATP-linked OCRs in the Control, LPS, and LPS + BMSC groups were  $481.89 \pm 92.77$ ,  $325.44 \pm 39.50$ , and  $442.56 \pm 82.35$ , respectively. The LPS group had lower ATP-linked OCR than the Control group ( $P < 0.05$ ). No significant

difference in ATP-linked OCR was observed between the Control and LPS + BMSC groups ( $P = 0.545$ ) or between the LPS and LPS + BMSC groups ( $P = 0.105$ ).

The mitochondrial maximal respiration capacities in the Control, LPS, and LPS + BMSC groups were  $744.11 \pm 60.85$ ,  $325.78 \pm 49.28$ , and  $539.00 \pm 67.91$ , respectively ( $P < 0.001$ ). The Control group had a higher level than the LPS + BMSC group, which had a higher level than the LPS group ( $P < 0.05$ ). Overall, these results showed that compared with the control group, the basic oxygen consumption, oxygen consumption for ATP synthesis, and the maximum oxygen consumption capacity in the LPS group were significantly reduced. This suggests that LPS stimulation can decrease the mitochondrial respiratory function of alveolar macrophages, while BMSC reversed the impaired basic respiratory function and partially restored the maximum respiratory function of the mitochondria.

### Changes in ROS induced by LPS in alveolar epithelial cells co-cultured with BMSCs

The changes in LPS-induced ROS in MLE-12 cells co-cultured with BMSCs are shown in Fig. 7. The fluorescence

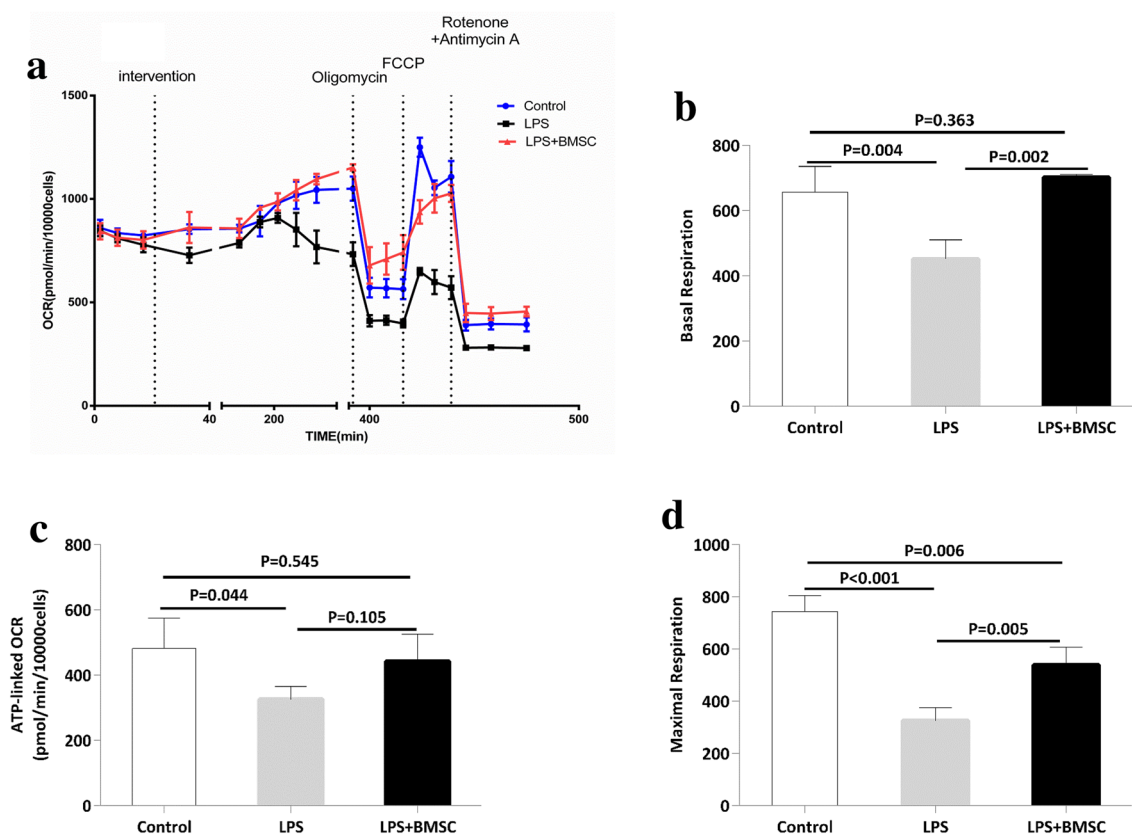


**Fig. 6** Changes in mitochondrial respiratory function induced by lipopolysaccharide (LPS) in macrophages co-cultured with bone marrow stem cells (BMSCs). **a** Changes in mitochondrial respiratory function measured by oxygen consumption rate (OCR) of macrophages (RAW264.7) in the Control, LPS, and LPS + BMSC groups.

**b** The basal mitochondrial OCR (pmol/min/10,000 cells) in the Control, LPS, and LPS + BMSC groups. **c** The ATP-linked OCR in the Control, LPS, and LPS + BMSC groups. **d** The mitochondrial maximal respiration capacity in the Control, LPS, and LPS + BMSC groups

signal was higher in the LPS group than in the Control and LPS + BMSC groups. The fluorescence signal was higher in the LPS + BMSC group than in the Control group, suggesting that LPS caused an elevation in ROS in alveolar epithelial cells, and that co-culture with BMSCs reduced the LPS-induced ROS generation.

The ATP concentration, as a measure of mitochondrial function, in the Control, LPS, and LPS + BMSC groups was  $25.15 \pm 0.17$ ,  $12.21 \pm 2.42$ , and  $18.79 \pm 1.62$ , respectively ( $P < 0.001$ ). The ATP concentration was the highest in the Control group, followed by the LPS + BMSC and LPS groups ( $P < 0.05$ ). The relative ATP levels in the Control, LPS, and LPS + BMSC groups were  $16.89 \pm 0.62$ ,  $8.60 \pm 0.47$ , and  $13.14 \pm 1.07$ , respectively ( $P < 0.001$ ). The relative ATP level was the highest in the Control group, followed by the LPS + BMSC and LPS groups ( $P < 0.05$ ).

### Mitochondrial respiratory function in alveolar epithelial cells

Figure 8 shows the respiratory function in alveolar epithelial cells. The changes in OCR in each group varied with time. The basal respiration OCRs in the Control, LPS, and LPS + BMSC groups were  $140.22 \pm 9.35$  pmol/min/10,000 cells,  $27.33 \pm 5.78$  pmol/min/10,000 cells, and  $102.33 \pm 6.66$  pmol/min/10,000 cells, respectively ( $P < 0.001$ ). The levels were the highest in the Control group, followed by the LPS + BMSC and LPS groups ( $P < 0.05$ ).

The ATP-linked OCRs in the Control, LPS, and LPS + BMSC groups were  $117.89 \pm 12.08$ ,  $4.33 \pm 6.64$ , and  $83.33 \pm 6.35$ , respectively ( $P < 0.001$ ). The levels were higher in the Control group than in the LPS + BMSC group, which was higher than in the LPS group ( $P < 0.05$ ). The maximal

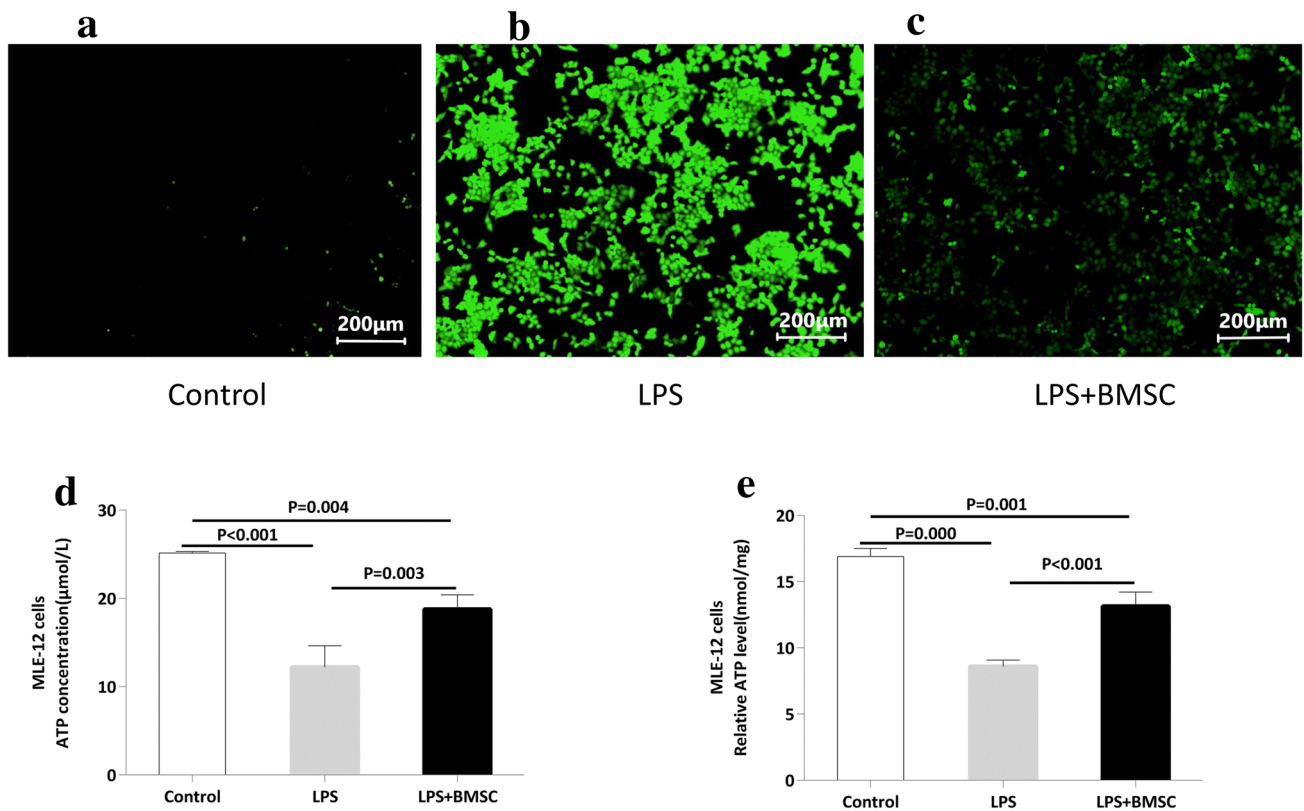


**Fig. 7** Changes in lipopolysaccharide (LPS)-induced reactive oxygen species (ROS) and mitochondrial function in alveolar epithelial cells (MLE-12) co-cultured with bone marrow stem cells (BMSCs). **a–c** ROS level indicated by green fluorescence in the Control, LPS,

and LPS + BMSC groups. **d** and **e** Mitochondrial function of alveolar epithelial cells in the Control, LPS, and LPS + BMSC groups represented by ATP concentration (**d**) and relative ATP level (**e**). (Color figure online)

OCRs in the Control, LPS, and LPS + BMSC groups were  $147.78 \pm 6.93$ ,  $100.44 \pm 20.92$ , and  $116.67 \pm 12.78$ , respectively ( $P = 0.02$ ). The LPS and LPS + BMSC groups had lower values than the Control group ( $P < 0.05$ ), but there was no significant difference between the LPS and LPS + BMSC groups ( $P = 0.225$ ).

These results showed that these three OCRs were reduced in the LPS group, suggesting that LPS stimulation decreased the mitochondrial respiratory function of alveolar epithelial cells, while BMSCs partially restored the impaired basal respiratory function and ATP production.

## Discussion

In this study, we used a mouse model of ARDS and an indirect co-culture system of mouse BMSCs with alveolar macrophages or epithelial cell lines to test cell metabolism and respiration, evaluate the mitochondrial function, and demonstrate those changes induced by LPS and alleviation caused by BMSCs. The study aimed to provide insights into the mechanisms involved in ARDS and its alleviation caused by

MSCs. The results showed that BMSCs improved the symptoms of ARDS in a mouse model alongside reversing the detrimental changes in IL-1 $\beta$ , TNF- $\alpha$ , and IL-10 inflammatory factors. In the cell-based assays, the BMSC co-culture also modified the inflammatory response and restored the mitochondrial respiration dysfunctions of alveolar epithelial cells and macrophages that were induced by LPS. ATP levels and ROS levels were changed, and impaired basal OCR, ATP-linked OCR, and maximal OCR were reversed by BMSCs.

The key point of this paper was that BMSCs improve the mitochondrial respiratory function of alveolar macrophages and alveolar epithelial cells, can increase the ATP level in alveolar macrophages and alveolar epithelial cells, reduce the ROS levels of alveolar macrophages and alveolar epithelial cells, improve cell dysfunction, and ultimately alleviate sepsis-induced ARDS. This study provides data about how BMSCs affect the specific changes in the mitochondrial respiratory function of alveolar macrophages caused by LPS stimulation, which has not been done before. There are few studies on the specific changes in the mitochondrial function of alveolar epithelial cells caused by LPS stimulation. The

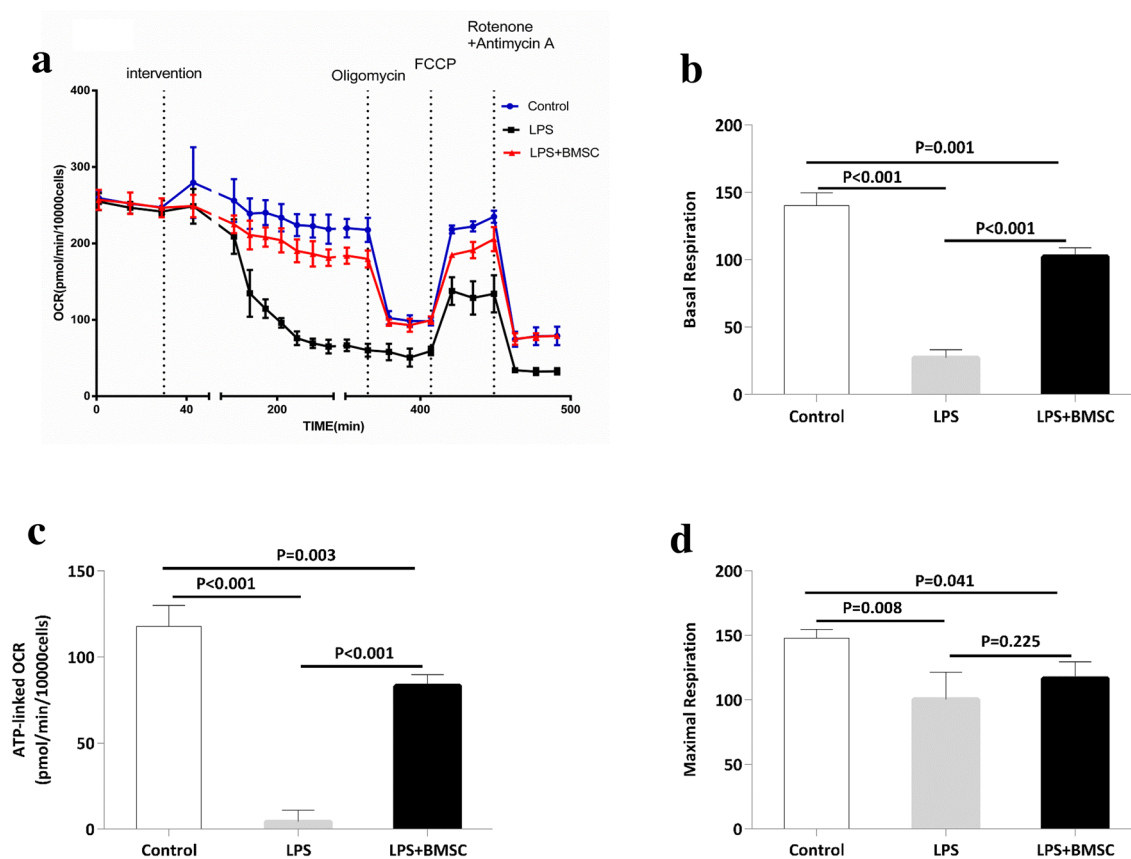


**Fig. 8** Mitochondrial respiratory function in alveolar epithelial cells (MLE-12). **a** Oxygen consumption rate (OCR) changes in the Control, LPS, and LPS + BMSC groups. **b** The basal respiration OCRs in

the Control, LPS, and LPS + BMSC groups. **c** The ATP-linked OCRs in the Control, LPS, and LPS + BMSC groups. **d** The maximal OCRs in the Control, LPS, and LPS + BMSC groups

effect of BMSCs on the mitochondrial function of alveolar epithelial cells induced by LPS stimulation has not been reported before.

The results of this study support previous studies that showed that MSCs could relieve ARDS symptoms in mice. Pedraza et al. confirmed that murine BMSCs administered in LPS-treated mice improved survival and reduced white cell influx to the lung, cyclooxygenase-2, nuclear factor  $\kappa$ B (NF- $\kappa$ B) expression, and neutrophil extracellular trap formation [29]. Human MSCs from Wharton's jelly could improve survival and increase the production of prostaglandin 2 and IL-10 in LPS-injected mice [30]. Human menstrual MSCs administered to LPS mice could decrease lung edema, decrease BALF IL-1 $\beta$ , and enhance lung repair [31]. Rats that had 100% O<sub>2</sub> for 48 h and cecal ligation puncture also were observed to have improved survival with the early administration of human umbilical cord MSCs [32]. Gupta et al. constructed an *Escherichia coli* endotoxin lung injury mouse model and confirmed that MSCs could alleviate lung injury and improve survival [33]. In their study, the MSCs were shown to inhibit pro-inflammatory TNF- $\alpha$  and enhance anti-inflammatory IL-10 secretion [33]. It was similar to our

results, but we found that TNF- $\alpha$  and IL-10 levels were all reduced by BMSCs in mouse lung tissue and BALF. On the other hand, in the macrophage co-culture experiments of our study, IL-10 levels in the cell supernatants were enhanced above that of the LPS group by BMSCs. These differences in different experiments highlight the complexity of the immune response. The timing of treatment and the measurements could be critical. The secretion of IL-10 has a compensatory effect on the inflammatory response. This was confirmed by the increase in IL-10 in the LPS group compared with the Control group. The animal experiments were tested 48 h after BMSC and LPS injection; at this time the pathological lung sections already confirmed that the degree of lung injury in the BMSC group was alleviated compared with the LPS group, so this might reduce the compensatory secretion of the anti-inflammatory factor IL-10 along with pro-inflammatory factors. Nevertheless, the cell experiments showed that at 24 h after treatment with BMSCs and LPS, a large amount of anti-inflammatory factor IL-10 was evident and had probably been induced by the BMSCs to respond to the inflammatory response. The results of this study also showed that co-culture with BMSCs did not directly affect

the secretion of inflammatory factors by alveolar epithelial cells stimulated by LPS, which suggests that BMSCs may affect the inflammatory response of the lung tissue through the macrophage pathway.

The research focus of our study was to investigate the role of mitochondrial dysfunction in ARDS and its alleviation by BMSCs. The generation of ATP by mitochondria requires a negatively charged matrix on the inner mitochondrial membrane that allows the passage of electrons over the electron transport chain. Stressors can disrupt the negative charge of the matrix, and the loss of the potential negative results in a failure of ATP production and the generation and release of ROS, which can lead to widespread damages [34]. Previous studies confirmed the role of mitochondria in response to inflammation. MSCs can donate their mitochondria to macrophages under oxidative stress via several extracellular ways, such as vesicle-mediated transport [35]. The transfer of mitochondria from MSCs promoted phagocytosis and suppressed pro-inflammatory cytokine secretion by human macrophages, mitigating lung injury *in vivo* [36]. The results of our study showed that BMSCs alleviated the increased ROS in macrophages and alveolar epithelial cells induced by LPS. The results also showed that the decreased ATP levels in macrophages and alveolar epithelial cells induced by LPS were reversed by BMSCs, which provided some clues that BMSCs maybe can reverse the damage of mitochondrial function induced by LPS.

Oxidation is an important source of energy for the efficient functioning of various organs, including the lung. Oxidation of NADH, pyruvate, or succinate in the body is done through the mitochondrial electron transport chain. We can use specific substrates and inhibitors to assess the independent mitochondrial ability to use an independent substrate and the specific function of using each compound [37]. OCR measurement is one of the preferred methods to assess cell mitochondrial function or dysfunction. Through testing controlled breathing oxygen consumption rate in the medium with the supplemental respiratory substrate, we can determine the oxygen consumption rate of the cells under basal respiratory conditions, the oxygen consumption to maintain ATP conversion, and the maximal capacity of the mitochondrial electron transport system [38]. In this study, we used the Seahorse XF96 bioenergy analyzer to detect the oxygen consumption of macrophages and alveolar epithelial cells under different intervention conditions, thereby demonstrating how the complex oxidative phosphorylation function of cells under different interventions was affected by specific substrate inhibitors, thus assessing the effect of BMSCs on the cellular mitochondrial function. We found that LPS stimulation could significantly reduce the basal oxygen consumption, oxygen consumption for ATP synthesis, and the maximum oxygen consumption capacity of macrophages' mitochondria,

confirming that stress factors can cause respiratory dysfunction of macrophages' mitochondria. We also found that BMSCs could significantly reverse the basic respiratory function damaged of macrophages' mitochondria, partially restore the maximum capacity of the mitochondrial electron delivery system. In the alveolar epithelial cells, we found that the basal oxygen consumption, the oxygen consumption for ATP synthesis, and the maximum oxygen consumption capacity were significantly reduced by LPS stimulation, confirming that stress factors can lead to significant respiratory dysfunction of alveolar epithelial cells mitochondria. BMSCs could partially restore the basal respiratory function of damaged alveolar epithelial cells and the oxygen consumption rate to maintain ATP conversion under basic conditions. Although the differences were not yet significant, a partial recovery trend also might appear in the impaired maximum capacity of the mitochondrial electron delivery system.

This study has some limitations. As a cell and animal model-based study, the results may not directly reflect the clinical situation. Further studies are needed to fully reveal the mechanisms involved.

BMSCs improved the ARDS symptoms in a mouse model by decreasing the inflammatory response. BMSCs co-culture with macrophages also modified the inflammatory response to LPS stimulation. Pulmonary immune cells such as macrophages and alveolar epithelial cells showed mitochondrial respiratory dysfunction induced by LPS, with the evidence of changed ROS, ATP, and OCR levels. Those dysfunctions were reversed, in part, by BMSCs. Therefore, our study suggests that BMSCs may be able to improve mitochondrial respiratory dysfunction of macrophages and alveolar epithelial cells so that they can alleviate ARDS.

**Author contributions** KZ was responsible for the animal and cell experiments, statistical analysis, and writing the paper. XZ was responsible for assisting cell culture and cell experiments. CZ was responsible for assisting the operation and animal experiments. ZH was responsible for assisting cell mitochondrial respiratory function testing. DL participated in acquisition, analysis, and interpretation of data. YG was responsible for the overall planning and design of the study. YD was responsible for assisting animal experiments and cell experiments. All authors read and approved the final manuscript.

**Funding** This study was supported by the National Natural Science Foundation of China (No. 81770067), Shanghai Municipal Science and Technology Commission Project (18411951100), and Shanghai Municipal Science and Technology Commission Project (18411967000).

**Data availability** All data generated or analyzed during this study are included in this published article. We declare that the materials described in the manuscript, including all relevant raw data, will be freely available to any scientist wishing to use them for non-commercial purposes, without breaching participant confidentiality.

## Compliance with ethical standards

**Conflict of interest** All authors declare that they have no conflict of interests.

**Ethical approval** All animal protocols were approved by the Institutional Animal Care and Use Committee of Ren Ji Hospital. All experiments were in accordance with the National Institutes of Health Guidelines for the Care and Use of Laboratory Animals.

**Informed consent** Not applicable.

## References

- McNicholas BA, Rooney GM, Laffey JG (2018) Lessons to learn from epidemiologic studies in ARDS. *Curr Opin Crit Care* 24:41–48. <https://doi.org/10.1097/mcc.0000000000000473>
- Wujtewicz M, Dylczyk-Sommer A, Aszkielowicz A et al (2020) COVID-19—what should anaesthesiologists and intensivists know about it? *Anaesthesiol Intensive Ther* 52:34–41. <https://doi.org/10.5114/ait.2020.93756>
- Yang X, Yu Y, Xu J et al (2020) Clinical course and outcomes of critically ill patients with SARS-CoV-2 pneumonia in Wuhan, China: a single-centered, retrospective, observational study. *Lancet Respir Med* 8:475–481. [https://doi.org/10.1016/s2213-2600\(20\)30079-5](https://doi.org/10.1016/s2213-2600(20)30079-5)
- Horie S, Gonzalez HE, Laffey JG, Masterson CH (2018) Cell therapy in acute respiratory distress syndrome. *J Thorac Dis* 10:5607–5620. <https://doi.org/10.21037/jtd.2018.08.28>
- Martin-Loeches I, Levy MM, Artigas A (2015) Management of severe sepsis: advances, challenges, and current status. *Drug Des Dev Ther* 9:2079–2088. <https://doi.org/10.2147/dddt.s78757>
- Fanelli V, Vlachou A, Ghannadian S et al (2013) Acute respiratory distress syndrome: new definition, current and future therapeutic options. *J Thorac Dis* 5:326–334. <https://doi.org/10.3978/j.issn.2072-1439.2013.04.05>
- Kellner M, Noonepalle S, Lu Q et al (2017) ROS signaling in the pathogenesis of acute lung injury (ALI) and acute respiratory distress syndrome (ARDS). *Adv Exp Med Biol* 967:105–137. [https://doi.org/10.1007/978-3-319-63245-2\\_8](https://doi.org/10.1007/978-3-319-63245-2_8)
- Fan E, Brodie D, Slutsky AS (2018) Acute respiratory distress syndrome: advances in diagnosis and treatment. *JAMA* 319:698–710. <https://doi.org/10.1001/jama.2017.21907>
- Carrasco Loza R, Villamizar Rodriguez G, Medel Fernandez N (2015) Ventilator-induced lung injury (VILI) in acute respiratory distress syndrome (ARDS): volutrauma and molecular effects. *Open Respir Med J* 9:112–119. <https://doi.org/10.2174/1874306401509010112>
- Girbes AR, Beishuizen A, Strack van Schijndel RJ (2008) Pharmacological treatment of sepsis. *Fundam Clin Pharmacol* 22:355–361. <https://doi.org/10.1111/j.1472-8206.2008.00606.x>
- Horie S, Laffey JG (2016) Recent insights: mesenchymal stromal/stem cell therapy for acute respiratory distress syndrome. *F1000Res*. <https://doi.org/10.12688/f1000research.8217.1>
- Wilson JG, Liu KD, Zhuo H et al (2015) Mesenchymal stem (stromal) cells for treatment of ARDS: a phase 1 clinical trial. *Lancet Respir Med* 3:24–32. [https://doi.org/10.1016/s2213-2600\(14\)70291-7](https://doi.org/10.1016/s2213-2600(14)70291-7)
- Nanchal RS, Truwit JD (2018) Recent advances in understanding and treating acute respiratory distress syndrome. *F1000Res*. <https://doi.org/10.12688/f1000research.15493.1>
- Cribbs SK, Matthay MA, Martin GS (2010) Stem cells in sepsis and acute lung injury. *Crit Care Med* 38:2379–2385. <https://doi.org/10.1097/CCM.0b013e3181f96f5f>
- Guillamat-Prats R, Artigas A (2019) Current status of stem cell therapy for sepsis and acute respiratory distress syndrome. In: *Innovations in cell research and therapy*. IntechOpen, London
- Wise AF, Williams TM, Kiewiet MB et al (2014) Human mesenchymal stem cells alter macrophage phenotype and promote regeneration via homing to the kidney following ischemia-reperfusion injury. *Am J Physiol Ren Physiol* 306:F1222–1235. <https://doi.org/10.1152/ajprenal.00675.2013>
- Vasandan AB, Jahnavi S, Shashank C et al (2016) Human mesenchymal stem cells program macrophage plasticity by altering their metabolic status via a PGE2-dependent mechanism. *Sci Rep* 6:38308. <https://doi.org/10.1038/srep38308>
- Allard B, Panariti A, Martin JG (2018) Alveolar macrophages in the resolution of inflammation, tissue repair, and tolerance to infection. *Front Immunol* 9:1777. <https://doi.org/10.3389/fimmu.2018.01777>
- Gregoire M, Uhel F, Lesouhaitier M et al (2018) Impaired efferocytosis and neutrophil extracellular trap clearance by macrophages in ARDS. *Eur Respir J*: <https://doi.org/10.1183/13993003.02590-2017>
- Kaczanowski S (2016) Apoptosis: its origin, history, maintenance and the medical implications for cancer and aging. *Phys Biol* 13:031001. <https://doi.org/10.1088/1478-3975/13/3/031001>
- Oh JY, Ko JH, Lee HJ et al (2014) Mesenchymal stem/stromal cells inhibit the NLRP3 inflammasome by decreasing mitochondrial reactive oxygen species. *Stem Cells* 32:1553–1563. <https://doi.org/10.1002/stem.1608>
- O'Halloran EB, Curtis BJ, Afshar M et al (2016) Alveolar macrophage inflammatory mediator expression is elevated in the setting of alcohol use disorders. *Alcohol* 50:43–50. <https://doi.org/10.1016/j.alcohol.2015.11.003>
- Mittal M, Siddiqui MR, Tran K, Reddy SP, Malik AB (2014) Reactive oxygen species in inflammation and tissue injury. *Antioxid Redox Signal* 20:1126–1167. <https://doi.org/10.1089/ars.2012.5149>
- Tang YL, Tang Y, Zhang YC et al (2005) Improved graft mesenchymal stem cell survival in ischemic heart with a hypoxia-regulated heme oxygenase-1 vector. *J Am Coll Cardiol* 46:1339–1350. <https://doi.org/10.1016/j.jacc.2005.05.079>
- D'Alessio FR (2018) Mouse models of acute lung injury and ARDS. *Methods Mol Biol* 1809:341–350. [https://doi.org/10.1007/978-1-4939-8570-8\\_22](https://doi.org/10.1007/978-1-4939-8570-8_22)
- Zhao YY, Gao XP, Zhao YD et al (2006) Endothelial cell-restricted disruption of FoxM1 impairs endothelial repair following LPS-induced vascular injury. *J Clin Invest* 116:2333–2343. <https://doi.org/10.1172/jci27154>
- Zhao YD, Huang X, Yi F et al (2014) Endothelial FoxM1 mediates bone marrow progenitor cell-induced vascular repair and resolution of inflammation following inflammatory lung injury. *Stem Cells* 32:1855–1864. <https://doi.org/10.1002/stem.1690>
- Zhu H, Guo ZK, Jiang XX et al (2010) A protocol for isolation and culture of mesenchymal stem cells from mouse compact bone. *Nat Protoc* 5:550–560. <https://doi.org/10.1038/nprot.2009.238>
- Pedrazza L, Cunha AA, Luft C et al (2017) Mesenchymal stem cells improves survival in LPS-induced acute lung injury acting through inhibition of NETs formation. *J Cell Physiol* 232:3552–3564. <https://doi.org/10.1002/jcp.25816>
- Condor JM, Rodrigues CE, Sousa Moreira R et al (2016) Treatment with human Wharton's jelly-derived mesenchymal stem cells attenuates sepsis-induced kidney injury, liver injury, and endothelial dysfunction. *Stem Cells Transl Med* 5:1048–1057. <https://doi.org/10.5966/sctm.2015-0138>

31. Xiang B, Chen L, Wang X et al (2017) Transplantation of menstrual blood-derived mesenchymal stem cells promotes the repair of LPS-induced acute lung injury. *Int J Mol Sci*: <https://doi.org/10.3390/ijms18040689>
32. Lee FY, Chen KH, Wallace CG et al (2017) Xenogeneic human umbilical cord-derived mesenchymal stem cells reduce mortality in rats with acute respiratory distress syndrome complicated by sepsis. *Oncotarget* 8:45626–45642. <https://doi.org/10.18632/oncotarget.17320>
33. Gupta N, Su X, Popov B et al (2007) Intrapulmonary delivery of bone marrow-derived mesenchymal stem cells improves survival and attenuates endotoxin-induced acute lung injury in mice. *J Immunol* 179:1855–1863. <https://doi.org/10.4049/jimmunol.179.3.1855>
34. Banoth B, Cassel SL (2018) Mitochondria in innate immune signaling. *Transl Res* 202:52–68. <https://doi.org/10.1016/j.trsl.2018.07.014>
35. Phinney DG, Di Giuseppe M, Njah J et al (2015) Mesenchymal stem cells use extracellular vesicles to outsource mitophagy and shuttle microRNAs. *Nat Commun* 6:8472. <https://doi.org/10.1038/ncomms9472>
36. Morrison TJ, Jackson MV, Cunningham EK et al (2017) Mesenchymal stromal cells modulate macrophages in clinically relevant lung injury models by extracellular vesicle mitochondrial transfer. *Am J Respir Crit Care Med* 196:1275–1286. <https://doi.org/10.1164/rccm.201701-0170OC>
37. Das KC (2013) Hyperoxia decreases glycolytic capacity, glycolytic reserve and oxidative phosphorylation in MLE-12 cells and inhibits complex I and II function, but not complex IV in isolated mouse lung mitochondria. *PLoS ONE* 8:e73358. <https://doi.org/10.1371/journal.pone.0073358>
38. Ruas JS, Siqueira-Santos ES, Amigo I et al (2016) Underestimation of the maximal capacity of the mitochondrial electron transport system in oligomycin-treated cells. *PLoS ONE* 11:e0150967. <https://doi.org/10.1371/journal.pone.0150967>

**Publisher's Note** Springer Nature remains neutral with regard to jurisdictional claims in published maps and institutional affiliations.